Gold Bull (2011) 44:223–230
DOI 10.1007/s13404-011-0034-5

ORIGINAL PAPER

Age-hardening characteristics of a dental low-carat gold alloy with dual hardener system of In and Cu

Hyo-Joung Seol · Seong-Woo Kweon · Su-Yeon Cho · Gwang-Young Lee · Yong Hoon Kwon · Hyung-Il Kim

Published online: 29 October 2011

Abstract The age-hardening characteristics of a dental low carat gold alloy with a dual hardener system of indium (In) and Cu (33.9 Au–26.2 Ag–20.28 Cu–9.8 Pd–7.8 In–2 Zn (at%)) were examined by observing the age hardenability and related phase transformation, microstructural changes and elemental distribution during the aging process at 400°C. The dual hardener system by the use of both In and Cu provided more powerful hardening effect compared to a single-hardener system of In or Cu, without the formation of a AuCu type ordered phase. The alloy showed apparent initial hardening, which was attributed to the pre-precipitation or zone formation by the help of quenched in excess vacancies. During the constant increase in hardness, the single parent phase separated into three phases, Au–Ag-based phase, Au–Cu-based phase containing Pd and In, and InPd-based phase, through a metastable state. Indium which was added as one of the hardeners induced initial grain boundary precipitation, followed by an expansion of the lamellar structure, which was responsible for softening. The alternative lamellar structure was composed of a Cu-rich layer (Au–Cu-based phase containing Pd and In) and an Ag-rich layer (Au–Ag-based phase) replaced partly by the InPd-based phase. Separation of the Ag-rich layer from the Cu-rich layer is based on the miscibility limit of Ag and Cu due to their eutectic property.

H.-J. Seol · S.-W. Kweon · S.-Y. Cho · G.-Y. Lee · Y. H. Kwon · H.-I. Kim (✉)
Dept. of Dental Materials,
School of Dentistry and Medical Research Institute,
Pusan National University,
Beomeo-Ri, Mulgeum-Eup,
Yangsan-Si, Gyeongsangnam-Do 626-814, South Korea
e-mail: seol222@pusan.ac.kr

Keywords Dual hardener system · Age-hardening characteristics · Phase transformation · Au–Ag–Cu–Pd–In · Alternative lamellar structure

Introduction

The recent increase in gold price has increased the demand for alternative dental alloys with lower Au contents. Dental low-carat gold alloys are alternative dental alloys with a higher Ag and Pd content compared to the high-carat gold alloy. The alloy composed of only Au, Ag, and Pd do not exhibit age hardenability, which is essential for dental crowns and bridges to withstand the occlusial force [1]. Accordingly, the well-known hardener, Cu, is added to dental low-carat gold alloys to achieve the age hardenability by forming a AuCu type ordered phase or by precipitating a Cu-based phase [2–6]. In such cases, if there is insufficient Au content for the formation of the AuCu phase or if Cu preferentially forms a stable phase with other elements in the as-cast state, the hardening effect of Cu will be unsatisfactory. Therefore, the extra Cu content, which could not act as a hardener, will exhibit preferential corrosion of the less noble phase. To avoid this, an element that exhibits a hardening effect together with sufficient tarnish and corrosion resistance was requested. Recently, indium (In) has been replacing Cu in an alternative Ag–Pd alloy because it exhibits age hardenability by the precipitation of an In-based phase from the Ag-rich matrix with sufficient tarnish and corrosion resistance [7, 8]. On the other hand, for dental low-carat gold alloys, the use of relatively large amounts of In as a hardener is unfamiliar because In is a minor ingredient that has been added only to improve the castability by decreasing the melting temperature. In recent studies on the age hardenability of dental

alloys, it was reported that the In-added Cu-free Ag–Pd–Au alloy (41.7 Ag–23 Pd–11.8 Au–16.7 In–6.8 Zn (at%)) aged at 350–450°C and the In-added Cu-free Au–Ag–Pd alloy (41.3 Au–39.8 Ag–13.7 Pd–5.2 In (at%)) aged at 450–550°C showed much lower age hardenability than the In-free Ag–Pd–Cu–Au alloy (53.9 Ag–20.8 Pd–14.1 Cu–6.7 Au–4 Zn (at%)) aged at 350–450°C [6, 9, 10]. By considering their results, which shows that In provides a weaker hardening effect than Cu, it was hypothesized that the adoption of a dual hardener system by In and Cu would have a more powerful hardening effect.

In the present study, a dental low carat Au–Ag–Cu–Pd alloy with a relatively high In content was studied. The hardening effects of the alloy were expected to be improved using a dual hardener system through the addition of In and Cu, but multiphase formation, which can be disadvantageous in terms of tarnish and corrosion resistance, was also a concern due to the relatively large In and Cu content. In this complicated alloy system, it is difficult to predict the process of phase transformation. The aim of this study is to elucidate the age-hardening characteristics of a dental low-carat gold alloy with a dual hardener system of In and Cu by characterizing the age hardenability and related phase transformation, microstructural changes, and elemental distribution.

Materials and methods

Specimen alloy

The alloy used in the present study was a yellow Au–Ag–Cu–Pd–In alloy used in crowns and bridge fabrications (Aurium52HN, Aurium research, USA), which belongs to type 3 alloy by the ISO classification (ISO 22674:2006(E)). Table 1 lists the chemical composition of the alloy. The initial shape of the specimen was plate-like with dimensions of 12×8×1 mm and was procured in a rolled and annealed state.

Hardness test

Before hardness testing, the specimens were solution-treated at 750°C for 15 min under an argon atmosphere and then rapidly quenched into ice brine to preclude thermal changes on cooling. They were subsequently aged at 400°C, as recommended by the manufacturer. All aging was done in a molten salt bath (25% KNO_3+30% KNO_2+25% $NaNO_3$+20% $NaNO_2$), followed by quenching into ice brine. Hardness measurements were made using a Vickers microhardness tester (MVK-H1, Akashi Co., Japan) with a load of 300 g-f and a dwell time of 10 s. Vickers hardness results were recorded as the average values of five measurements.

Table 1 Chemical composition of the alloy

Composition	Au	Ag	Cu	Pd	In	Zn	Ir
wt.%	51.9	22	10	8.07	7	1	0.03
at%	33.9	26.2	20.28	9.8	7.8	2	0.02

X-ray diffraction study

For the X-ray diffraction (XRD) study, powder specimens which passed through a 300-mesh screen were obtained by filing the plate-like samples. After being vacuum sealed in a silica tube and solution-treated at 750°C for 15 min, they were isothermally aged at 400°C for various periods of time in a molten salt bath, and then quenched into ice brine. The X-ray diffraction profiles were recorded by an X-ray diffractometer (XPERT-PRO, Philips, Netherlands). The X-ray diffractometer was operated at 30 kV and 40 mA, using nickel-filtered Cu Kα radiation. The scanning rate of a goniometer was 2° (2θ/min).

Field emission scanning electron microscopic observations

For the field emission scanning electron microscopic observations (FE-SEM), the plate-like samples were subjected to the required heat treatment and then prepared by utilizing standard metallographic techniques. A freshly prepared aqueous solution of 10% potassium cyanide and 10% ammonium persulfate ($(NH_4)_2S_2O_8$) was used for the final etching of the samples. The specimens were examined at 15 kV using a field emission scanning electron microscope (JSM-6700 F, JEOL, Japan).

Energy dispersive spectrometer analysis

Energy dispersive spectrometer (EDS) analysis was done to observe the distributional changes of each element in the alloy during the aging process. The specimens were prepared in the same manner as was used for the scanning electron microscopic observations. Energy dispersive spectrometer analysis was performed using a field emission scanning electron microscope (JSM-6700 F, JEOL, Japan) equipped with an energy dispersive X-ray spectrometer (INCA x-sight, Oxford Instruments Ltd., UK).

Results and discussion

Age-hardening behavior

Figure 1 shows the isothermal age hardening curve of the alloy solution-treated at 750°C for 15 min and aged at

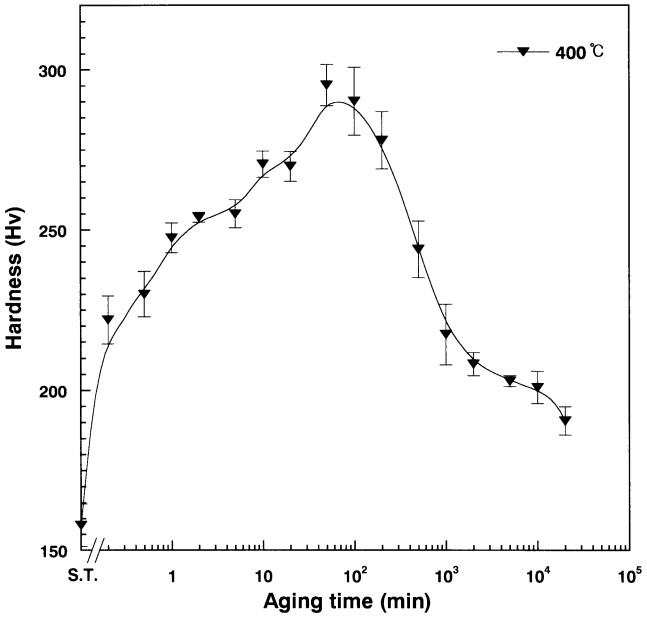

Fig. 1 Isothermal age hardening curve of the alloy aged at 400°C

400°C for various times. The hardness increased apparently from 158 to 222 Hv after 12 s aging. Therefore, it was supposed that the quenched in excess vacancies attributed to atomic diffusion, resulting in an instant increase in hardness.

It was reported that the addition of In to AuCu alloy reduced the age hardenability at low temperatures, which is controlled by the number of free vacancies and diffusion [11]. Although In has a low melting temperature, which is advantageous for vacancy diffusion, its large binding energy with vacancies decreases the number of effective free vacancies for diffusion, which retards the age hardenability at low temperatures [11–13]. On the other hand, in the present study, even with a relatively large In content, the alloy showed apparent initial hardening, which was attributed to quenched in excess vacancies. This might be attributed to the Pd content, which tends to form a stable phase preferentially with In, as will be discussed in the XRD studies [1].

After 12 s, the hardness increased constantly, and the maximum hardness, 295 Hv, was obtained at an aging time of 50 min. The hardness began to decrease considerably until an aging time of 2,000 min. Subsequently, the decreasing rate of hardness was retarded until an aging time of 20,000 min. The maximum hardness, 295 Hv, obtained in the present study was slightly higher than the value obtained in the In-free Ag-Pd-Cu-Au alloy aged at 350–450°C (280 Hv) and much higher than the value, 220 Hv, obtained in the Cu-free Ag–Pd–Au–In alloy aged at 350–450°C and the Cu-free Au–Ag–Pd–In alloy aged at 450–550°C [6, 9, 10]. Hence, the dual hardener system by the use of both In and Cu was believed to have provided more powerful hardening effect compared to a single-hardener system of In or Cu.

Phase transformation

To understand the mechanism of age hardening, the phase transformation with aging was observed by XRD. Figure 2 shows the variations of the XRD pattern during 400°C isothermal aging. In the solution-treated specimen, a face-centered cubic (fcc) single phase was obtained. The fcc phase (α) had a lattice parameter of a_{200}=0.40 nm. By aging the solution-treated specimen for 20,000 min, the parent fcc α phase was transformed to an fcc α_1 phase with slight increase in the lattice parameter, a_{200}=0.406 nm by precipitating the CsCl-type body-centered cubic (bcc) β phase with a lattice parameter of a_{211}=0.321 nm, and the fcc α_2 phase with a_{200}=0.387 nm. The InPd phase was reported to be a CsCl type bcc structure with a lattice parameter of a=0.325 nm [14]. From the alloy composition and lattice parameter of each phase, the β and α_2 phase was to be respectively, the InPd-based phase and Au–Cu-based phase containing Pd and In. The α_2 phase had a similar lattice parameter to that of Pd (a=0.38908 nm) even with a relatively high Cu with small atomic size [15]. This was attributed to the In content with a relatively large atomic

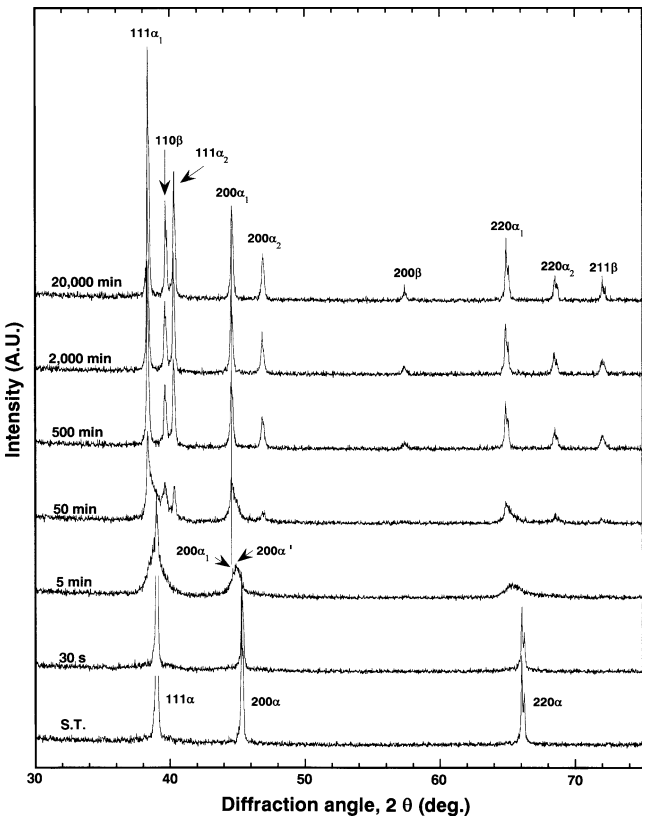

Fig. 2 Variations of the XRD patterns as a function of isothermal aging time at 400°C

size in the α_2 phase [15] as shown in the EDS results. From the above, the age hardenability of the alloy was related to phase separation into three phases of the Au–Ag-based phase, Au–Cu-based phase containing Pd and In, and InPd-based phase. In a study on the age-hardening mechanism of the 41.7 Ag–30.15 Au–20.9 Cu–4.7 Pd–1.1 In (at%) alloy aged at 400°C, the AuCu-type ordered-phase attributed to an increase in hardness [16]. In the present study, although the Au and Cu content was similar to the above alloy, the formation of the AuCu-type ordered-phase was not observed.

The changes in the XRD patterns during isothermal aging at 400°C were examined with respect to the isothermal age hardening curve at 400°C (Fig. 1). The hardness increased apparently from 158 to 222 Hv after 12-s aging. On the other hand, there were no apparent changes in the XRD pattern until 30-s aging. It is known that pre-precipitation or zone formation does not result in a shift in the fundamental diffraction peaks [17, 18]. Therefore, the quenched in excess vacancies assisted the diffusion of the solute, resulting in pre-precipitation or zone formation. At an aging time of 5 min, the hardness increased to 255 Hv. In the corresponding XRD pattern, the diffraction peaks of the α phase became broader with a concomitant decrease in peak intensity. The (200) α peak shifted toward a lower diffraction angle side and was divided into two, indicating the coexistence of a metastable phase (α') with the final stable phase (α_1). Therefore, the final α_1 phase formed through a metastable state by the precipitation of α_2 and β. The metastable phase has a lattice parameter between the parent phase and final stable phase. Therefore, the formation of a metastable phase must have minimized the accumulation of the lattice strain in the matrix by reducing the gap in the lattice parameters among the parent and product phases.

At an aging time of 50 min, when the maximum hardness value, 295 Hv, was obtained, the 110 β and 111 α_2 peaks became strong and the parent α phase was in the process of transforming into the stable α_1 phase. The asymmetrically broad (200) α_1 peak indicated that the metastable α phase still remained. This suggests that both the formation of the metastable α' phase and its subsequent transformation into the stable α_1 phase attributed to an increase in hardness. On the other hand, from the fact that a further increase in hardness stopped at 50 min when the phase transformation was still in progress, it was supposed that some microstructural changes, which are related to softening were already initiated, as will be shown in the FE-SEM observations.

By further aging until 500 min when the peak hardness decreased to 244 Hv, the parent 111 α peak disappeared and the phase transformation was almost complete. Until an aging time of 20,000 min when a drastic decrease in hardness to 190 Hv had occurred, the broad diffraction peaks became sharp. From the above, during the period of the hardness decrease, there was no apparent change in the XRD patterns except for peak sharpening. This peak broadening and then sharpening implies the introduction and then release of lattice strain in the matrix, resulting in softening [19–22]. Therefore, the microstructural changes related to the release of lattice strain were supposed in the later stage of the aging process.

Microstructural changes

FE-SEM observations were performed to clarify the microstructural changes occurring during the hardness changes. Figure 3 shows FE-SEM micrographs of ×1,000 and ×40,000 for the specimen solution treated at 750°C for 10 min (a) and aged at 400°C for the following time periods: 50, 500, 2,000, and 20,000 min. In the solution-treated specimen (Fig. 3a), a single phase was obtained, as indicated in the XRD pattern. In dental alternative alloys containing high Pd levels, it is difficult to obtain a single-phase solid solution because Pd preferentially forms an additional stable phase with In or Cu in the form of a particle-like structure [6, 9, 10]. In such a case, the age hardenability is obtained only by the remaining In or Cu which did not constitute the particle-like structure [6, 9, 10]. In the present alloy with a dual hardener system of In and Cu, however, the particle-like structure was not formed in the solution-treated state. Hence, the total amounts of In and Cu might have participated in the phase transformation process. This also imparted powerful age hardenability to the present alloy system compared to that with a single-hardener system of In or Cu, as mentioned above [6, 9, 10].

In the specimen aged for 50 min (B) when the maximum hardness value was obtained, no change in the grain interior was observed, and the limited area of the grain boundaries was replaced by the lamellar structure. In the corresponding XRD pattern, the parent phase was in the process of transforming into the stable phases through the metastable state, resulting in a multiphased matrix. Considering the gap in the lattice parameters among the existing phases, the grain interior was thought to have apparent internal strain. Therefore, to release the internal lattice strain, the lamellar-forming grain boundary reaction, which is a well-known softening mechanism, was initiated, as will be further mentioned [3, 23, 24].

By further aging until 500 min (C), besides expansion of the grain boundary lamellar structure, the grain interior structure changed into a complex structure with a finer nature than the grain boundary structures, as shown in (C-2). By further aging for 2,000 min (D), the grain boundary lamellar structure covered almost the entire matrix, and the complex grain interior

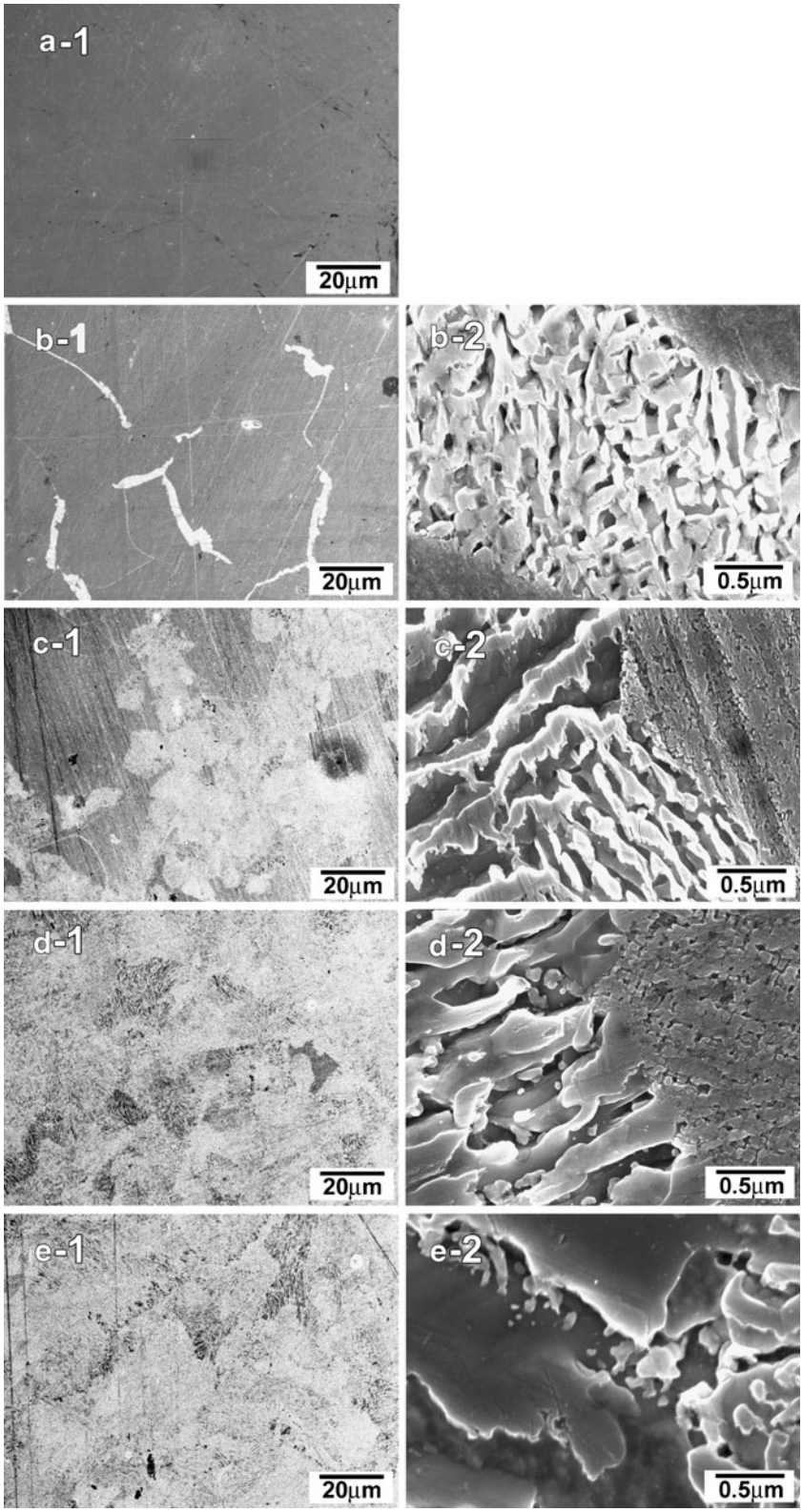

Fig. 3 FE-SEM micrographs of specimens **a** solution-treated at 700°C for 10 min and aged at 400°C for **b** 50 min, **c** 500 min, **d** 2,000 min, and **e** 20,000 min (*1*) ×1,000, (*2*) ×40,000

structure was further coarsened. At an aging time of 20,000 min, the inter-lamellar spacing was further coarsened (E-2), which corresponded to a further decrease in hardness.

From the above, during the hardness decrease, there were apparent microstructural changes. The expansion of the lamellar structure and further coarsening reduces the interphase boundaries containing lattice strain, which

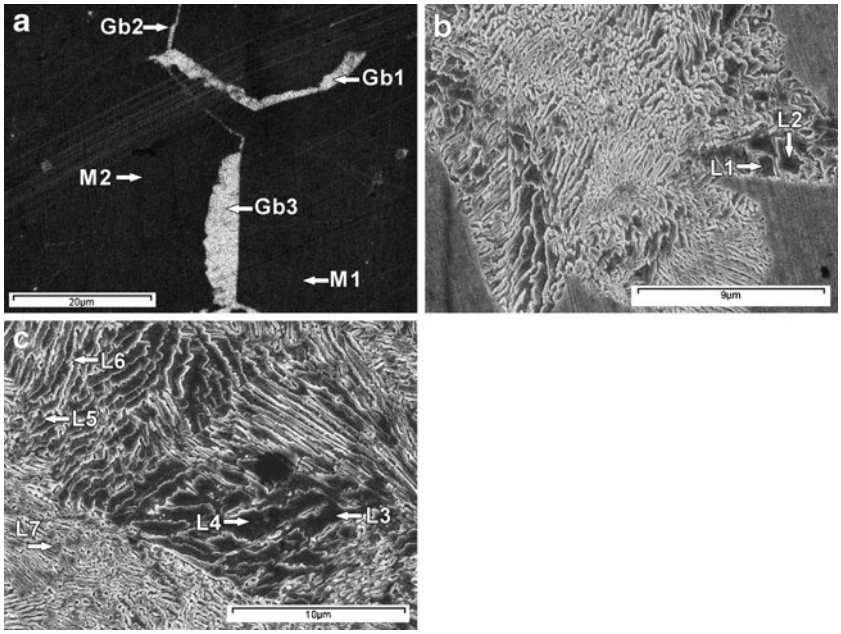

Fig. 4 FE-SEM micrographs of specimen aged at 400°C for **a** 50 min, **b** 500 min, and **c** 20,000 min: features *arrowed M*, *Gb*, and *L* are discussed in text

results in softening [3, 23, 24]. The decreasing rate in hardness was proportional to the replacing ratio of the matrix by the lamellar structure considering the FE-SEM results and the hardness changed from 50 min until 2,000 min. On the other hand, further coarsening of the interlamellar spacing after the entire replacement of the lamellar structure did not result in severe softening as much as expansion of the lamellar structure.

Changes in the elemental distribution

The changes in elemental distribution with aging time were examined by EDS. Figure 4 shows FE-SEM micrographs of the specimen aged at 400°C for 50 min (a) when the maximum hardness, 295 Hv, was obtained, 500 min; (b) when the hardness decreased to 244 Hv, and 20,000 min; (c) when drastic softening down to 190 Hv was observed. The regions analyzed, as marked by the arrow, were the matrix (M), grain boundary precipitates (Gb), and each layer of the lamellar structures (L). The results are shown in Table 2 A–C regions. In the specimen aged for 50 min (A), the grain boundary lamellar precipitates (Gb) showed apparently less Cu with slightly more Pd and In with or without an increase in Ag compared to the alloy composition listed in Table 1. The Au content did not show apparent changes, and the Zn content did not show consistency. The corresponding XRD results showed that the single parent phase was in the process of separating into three phases; Au–Ag-based phase, Au–Cu-based phase containing Pd and In, and InPd-based phase. By considering the XRD results together with the EDS results, such a change at Gb was obtained from both the Au–Ag-based phase and InPd-based phase, as will be further discussed. Considering the large sampling spot size and that Ag is one of the major components, the grain boundary precipitates are thought to be composed mainly of In and Pd. These results suggest that In, which was added as a hardener, induced the initial grain boundary precipitation which is responsible for softening. Several studies have reported that the initial grain boundary precipitation occurred mainly by In and Pd in dental gold alloys which were hardened by formation of the AuCu I phase [16, 25]. The multiphased matrix (M) showed the same composition as that of the alloy of the solution-treated state due to the large sampling spot size, which covers all the submicroscopic precipitates in the matrix.

Table 2 EDS analysis at the regions marked in Fig. 4a–c

	Au	Ag	Cu	Pd	In	Zn
A region (at %)						
Gb1	32.6	31.1	14	11.6	9.3	1.4
Gb2	33.3	25.7	14.4	12.2	9.9	4.5
Gb3	33.5	26.4	14.1	12.3	10.2	3.5
M1	33.3	24.3	20.2	9.3	8	4.9
M2	36.2	24.7	20.8	8.0	7.5	2.8
B region (at %)						
L1	31.6	16.1	26.3	12.8	10.4	2.8
L2	34.6	30.4	12.2	11.2	10	1.6
C region (at %)						
L3	30.5	14	27.8	15.8	8.5	3.4
L4	29.1	31.6	9.9	13.5	12.6	3.3
L5	31	10.4	26.6	17	10	5
L6	27.7	21.3	13.1	19.3	11.6	7
L7	34.7	36.2	9.8	8.9	7.7	2.7

In the specimen aged for 500 min (B), the (L1) layer of the coarse lamellar structure had a lower Ag content and higher Cu content, and the neighboring (L2) layer had a higher Ag content and lower Cu content compared to the alloy composition listed in Table 1. In and Pd increased slightly in both layers. Such a tendency was also observed in the specimen aged for 20,000 min (C). The coarse two neighboring layers (L3,4) had a slightly higher In and Pd content, and were distinguished by the contradictory content of Ag and Cu. Considering the XRD results together, the (L3) layer of the coarse lamellar was composed of the Au–Cu-based phase containing Pd and In, and the (L4) layer was composed of both the Au–Ag-based phase and the InPd-based phase. The finer layer (L5) and neighboring layer (L6) also showed a similar result to that of the (L3) and (L4) layers.

Besides the Ag-rich region with slightly increased In and Pd content, there was also the Ag-rich region (L7) with slightly less Pd and In. From such a discrepancy of the In and Pd content in the Ag-rich regions, it was suggested that the Ag-rich layer, which was composed of the Au–Ag-based phase, was replaced partly by the InPd-based phase, and was separated from the Cu-rich layer composed of the Au–Cu-based phase containing Pd and In. The separation of the Ag-rich layer from the Cu-rich layer is based on the miscibility limit of Ag and Cu due to their eutectic property according to the binary phase diagram of Ag and Cu [1]. On the other hand, Au has complete solubility with both Ag and Cu at all atomic ratios, which corresponds to a relatively constant Au content in both the Ag-rich and Cu-rich layers [1].

Summary

The age hardening characteristics of a dental low carat gold alloy with a dual hardener system of In and Cu (33.9 Au–26.2 Ag–20.28 Cu–9.8 Pd–7.8 In–2 Zn (at%)) was examined by observing the age hardenability and related phase transformations, microstructural changes and elemental distribution during aging at 400°C. The results are as follows.

1. The dual hardener system of In and Cu provided a powerful hardening effect without the formation of the AuCu-type ordered phase in the Au–Ag–Cu–Pd alloy with a relatively high In content.
2. The alloy showed apparent initial hardening that was attributed to pre-precipitation or zone formation by the aid of quenched in excess vacancies.
3. During the constant increase in hardness, the single parent phase separated into three phases, Au–Ag-based phase, Au–Cu-based phase containing Pd and In, and InPd-based phase, through a metastable state.
4. Indium added as a hardener induced initial grain boundary precipitation, followed by an expansion of the lamellar structure, which is responsible for softening.
5. The miscibility limit of Ag and Cu resulted in the formation of alternative lamellar structure which was composed of the Cu-rich layer (Au–Cu-based phase containing Pd and In) and the Ag-rich layer (Au–Ag-based phase) replaced partly by the InPd-based phase.

References

1. Massalski TB (1990) Binary alloy phase diagrams, 2nd edn. ASM International, Materials Park, pp 12–13 (Ag-Au), 28–29 (Ag-Cu), 72–74 (Ag-Pd), 358–362 (Au-Cu), 409–410 (Au-Pd), 2271–2273 (In-Pd)
2. Yasuda K, Ohta M (1982) Difference in age-hardening mechanism in dental gold alloys. J Dent Res 61:473–479
3. Yasuda K (1987) Age-hardening and related phase transformations in dental gold alloys. Gold bull 20:90–103
4. Yasuda K, Hisatsune K (1993) Microstructure and phase transformations in dental gold alloys. Gold bull 26:50–66
5. Hisatsune K, Shiraishi T, Takuma Y, Tanaka Y, Luciano RH (2007) Two different types of age-hardening behaviors in commercial dental gold alloys. J Mater Sci Mater Med 18:577–581
6. Seol HJ, Kim GC, Son KH, Kwon YH, Kim HI (2005) Hardening mechanism of an Ag-Cu-Pd-Au dental casting alloy. J Alloys Compd 387:139–146
7. Hattori M, Tokizaki T, Matsumoto M, Oda Y (2010) Corrosion properties of Ag-Au-Cu-Pd system alloys containing indium. Bull tokyo dental coll 51:7–13
8. Cho SY, Lee GY, Kwon YH, Kim HI, Seol HJ (2011) Age-hardening characteristic of a Cu-free Ag-Pd alloy containing high In. J Korean Res Soc Dent Mater 38:91–100
9. Seol HJ, Son KH, Yu CH, Kwon YH, Kim HI (2005) Precipitation hardening of a Cu-free Au-Ag-Pd-In dental alloy. J Alloys Compd 402:130–135
10. Lee HK, Moon HM, Seol HJ, Lee JE, Kim HI (2004) Age hardening by dendrite growth in a low-gold dental casting alloy. Biomaterials 25:3869–3875
11. Ohta M, Shiraishi T, Nakagawa M, Matsuya S (1994) Dental gold alloys with age-hardenability at intraoral temperature. J Mater Sci 29:2083–2086
12. Ouchida R, Shiraishi T, Nakagawa M, Ohta M (1995) Effects of Au/Cu ratio and gallium content on the low-temperature age-hardening in Au-Cu-Ga alloys. J Mater Sci 30:3863–3866
13. Shewmon P (1989) Diffusion in solids, 2nd edn. TMS, Warrendale, PA, p 147
14. Hellner E, Laves F (1947) Kristallchemie des In und Ga in Legierungen mit einigen Übergangselementen (Ni, Pd, Pt, Cu, Ag und Au). Z Naturforschg 2a:177–183
15. Cullity BD (1978) Elements of X-ray diffraction, 2nd edn. Addison-Wesley, Massachusetts, pp 506–507

16. Jeon GH, Kwon YH, Seol HJ, Kim HI (2008) Hardening and overaging mechanisms in an Au-Ag-Cu-Pd alloy with In additions. Gold bull 41:302–308
17. Ohta M, Hisatsune K, Yamane M (1979) Age-hardening of Ag-Pd-Cu dental alloy. J Less-common Metals 65:11–21
18. Shiraishi T, Ohta M (2002) Age-hardening behaviors and grain boundary discontinuous precipitation in a Pd-free gold alloy for porcelain bonding. J Mater Sci Mater Med 13:979–983
19. Tanaka Y, Udoh K, Hisatsune K, Yasuda K (1998) Early stage of ordering in stoichiometric AuCu alloy. Mater Trans JIM 39:87–94
20. Kim HI, Ahn HK, Lee HK, Hisatsune K, Seol HJ, Takuma Y (1999) Isothermal age-hardening behaviour in a multi-purpose dental casting alloy. Dent Mater J 18:314–323
21. Suryanarayana C, Norton MG (2003) X-ray diffraction: a practical approach, 1st edn. Springer, New York, pp 207–210
22. Kawashima I, Ohno H, Sarkar NK (2000) Effect of Pd or Au addition on age-hardening in AgMn-based alloys. Dent Mater 16:75–79
23. Hisatsune K, Udon K, Nakagawa M (1990) Aging behaviour in a dental low carat gold alloy and its relation to CuAuII. J Less-common Metals 160:247–258
24. Hisatsune K, Udon KI (1991) Age-haradening characteristics in an AuCu-14 at.%Ag alloy. J Alloys Compd 176:269–283
25. Seol HJ, Noh DJ, Lee SH, Kwon YH, Kim HI (2008) Age-hardening by the formation of metastable phases in an In-added Au-Ag-Cu-Pd alloy. Materials Characterization 59:1190–1195